Journal of Nuclear Materials 492 (2017) 195–203

Contents lists available at ScienceDirect

Journal of Nuclear Materials

journal homepage: www.elsevier.com/locate/jnucmat

Irradiated microstructure of U-10Mo monolithic fuel plate at very high fission density

J. Gan*, B.D. Miller, D.D. Keiser Jr., J.F. Jue, J.W. Madden, A.B. Robinson, H. Ozaltun, G. Moore, M.K. Meyer

Idaho National Laboratory, P. O. Box 1625, Idaho Falls, ID 83415, USA

ARTICLE INFO

Article history:
Received 12 April 2017
Received in revised form
22 May 2017
Accepted 23 May 2017
Available online 26 May 2017

ABSTRACT

Monolithic U-10Mo alloy fuel plates with Al-6061 cladding are being developed for use in research and test reactors as low enrichment fuel (<20% U-235 enrichment) as a result of its high uranium loading capacity compared to that of U-7Mo dispersion fuel. These fuel plates contain a Zr diffusion barrier between the U-10Mo fuel and Al-6061 cladding that suppresses the interaction between the U-Mo fuel foil and Al alloy cladding that is known to be problematic under irradiation. Different methods have been employed to fabricate monolithic fuel plates, including hot-rolling with no cold-rolling. L1P09T is a hot-rolled fuel plate irradiated to high fission density in the RERTR-9B experiment. This paper discusses the TEM characterization results for this U-10Mo/Zr/Al6061 monolithic fuel plate (~59% U-235 enrichment) irradiated in Advanced Test Reactor at Idaho National Laboratory with an unprecedented high local fission density of 9.8E+21 fissions/cm^3. The calculated fuel foil centerline temperature at the beginning of life and the end of life is 141 and 194 °C, respectively. TEM lamellas were prepared using focus ion beam lift-out technique. The estimated U-Mo fuel swelling, based on the fuel foil thickness change from SEM, is approximately 76%. Large bubbles (>1 μm) are distributed evenly in U-Mo and interlink of these bubbles is evident. The average size of subdivided grains at this fission density appears similar to that at 5.2E+21 fissions/cm^3. The measured average Mo and Zr content in the fuel matrix is ~30 at% and ~7 at%, respectively, in general agreement with the calculated Mo and Zr from fission density.

1. Introduction

The high performance research and test reactor fuel development program (HPRR-FD) aims to develop low enrichment (<20% ^{235}U) U-Mo fuels to ensure a safe and secured use of research and test reactors worldwide. It is an important program on global nuclear non-proliferation. Microstructural development under irradiation can have a strong effect on the fuel and material performance in reactors. Significant efforts have been put into developing a comprehensive understanding of the U-Mo fuel microstructural evolution under irradiation. Plate type of fuels either in dispersion or monolithic configuration is the most popular fuel format for these reactors. The advantage for a monolithic fuel plate is its higher uranium loading capacity comparing to a dispersion fuel, which allows the use of U-10Mo that is thermodynamically more stable than U-7Mo based on the time-temperature-transformation (TTT) diagram [1,2]. More information on these types of plate fuels can be found in the literature [3–5]. To suppress the interaction between the U-Mo fuel and the Al 6061 cladding, a thin Zr foil (25 μm) is added as a diffusion barrier between the U-Mo and Al 6061. Different methods have been employed to fabricate monolithic fuel plates for testing in the Advanced Test Reactor (e.g., Zr-bonded U-10Mo foils have been produced using hot-rolling followed by cold-rolling, or just hot-rolling). A comprehensive microstructural characterization is required to investigate the radiation stabilities of the fuel foil and relevant interaction product phases at the fuel/cladding interfaces for fuel fabricated in different ways.

The previous work on TEM characterization of the irradiated microstructure for U-7Mo dispersion fuels with fission densities up to 6.31 × 10^{21} fissions/cm^3 can be found in the literature [6–9]. General observations on the irradiated microstructure in U-Mo fuels could be described as following. At low fission densities, fuel

* Corresponding author. Characterization and Advanced PIE Division, Idaho National Laboratory, P.O. Box 1625, Idaho Falls, ID 83415-6188, USA.
E-mail address: Jian.Gan@inl.gov (J. Gan).

http://dx.doi.org/10.1016/j.jnucmat.2017.05.035
0022-3115/

swelling is dominated by solid fission product and the role of fission gas is insignificant. As the fission density increases, fission gas bubbles develop in two modes in parallel with large ones initiated at grain boundaries and the small ones formed gas bubble superlattice (GBS) within the U-Mo grains. At a fission density of approximately 3×10^{21} fissions/cm^3, it appears the GBS bubbles reach a steady state with average bubble size around 3.5 nm and a superlattice constant of approximately 11.5 nm for a face-centered-cubic (fcc) superlattice. As fission density further increases, the average size of fine bubbles and superlattice constant remains constant within the measurement uncertainty while the width of the large bubble region expands from the original grain boundaries into the U-Mo grain interior. At fission densities around approximately 5×10^{21} fissions/cm^3, it appears two processes leading to the destruction of GBS. One is the coalescence of the fine bubbles within the grains and the other is the further expansion of the large bubble region into the grain interior. Pockets of fine superlattice bubbles survive with an area fraction of roughly 10–20%. Grain subdivision at this fission density becomes evident and the original large grains (~5 μm) are divided into much smaller grains (~200 nm). There is no microstructural evidence showing the preferential bubble accumulation at these newly developed low-misfit-angle subdivided grain boundaries. At high fission density of ~6×10^{21} fissions/cm^3, the large bubble region initiated from the original grain spread across and become the dominant microstructure in U-Mo fuel grains. The superlattice bubble regions are nearly completely consumed although there are still few scattered small pockets of superlattice bubbles that can be found. A significant amount of fission products precipitate at these large bubbles (>500 nm) and form an amorphous shell around these bubbles with some fission products appearing as amorphous precipitates attached inside the bubble.

The microstructural data of TEM characterization for the irradiated U-10Mo fuel in a monolithic fuel plate is still lacking. This work presents the recent results of TEM characterization of the irradiated U-10Mo contained in a fuel plate fabricated using hot-rolling followed by hot isostatic pressing (HIP). It had the highest fission density ever achieved to date. These new results are important to improve the understanding of the fundamental mechanism governing the microstructural evolution in the U-Mo fuels under the reactor irradiation condition dominated by the energetic fission fragments (~80 MeV), and any possible impacts of using different methods to fabricate the fuel. This work suggests that the speculation of the U-Mo fuel microstructural evolution at very high fission density based on the previous results obtained at the relatively lower fission densities could be misleading.

2. Experiment

The monolithic U-10Mo/Zr/Al6061 fuel plate (ID: L1P09T, 59% enriched) was fabricated using first a hot-rolling process to apply the Zr diffusion barrier to the foil followed by a HIP process to apply the AA6061 cladding. Fig. 1 describes the hot-rolling process for different Zr-clad U-10Mo foils that ended up in monolithic fuel plates that were eventually tested in the RERTR-9 experiment, which was divided into two parts–A and B. Fuel plate L1P09T was irradiated in the RERTR-9B part [10]. Two HIP runs (HIP-9B-24 and HIP-9B-23) were conducted at the same temperature and pressure in order to fabricate all the HEU bearing mini-plates for the RERTR-9B irradiation. The HIP runs were carried out at 560 °C and 15000 psi for 90 min. The heating and cooling rate were controlled by a Microstar programmable controller. The ramp rate was 280 °C per hour. The initial pressure of the vessel was 800 psi and the compressor was turned on at 350 °C so that the vessel pressure reached 15000 psi at 560 °C. After holding at 560 °C for 90 min, the vessel was cooled down and the pressure was decreased to 2000 psi before manually vented to atmosphere pressure at 50 °C.

In the Hot Fuel Examination Facility, a small slice was cut was made from the irradiated fuel plate and sent to the Electron Microscopy Laboratory for analysis. It was calculated that during irradiation this sample had been exposed to a local fuel centerline temperature of approximately 141 °C at the beginning of life (BOL) and 194 °C at the end of life (EOL) to a fission density of 9.8×10^{21} fissions/cm^3 [11]. This fission density is 55% higher than the highest fission density (6.3×10^{21} f/cm^3) in the previously investigated U-7Mo dispersion fuel [8]. The standard met-mount sample was prepared using a glovebox with final surface finish of 1.0 μm polishing compound. Scanning electron microscopy (SEM) analysis was performed using both a dual-beam focused ion beam (FIB) unit and a JEOL-7000F SEM system. Five site-specific TEM lamellas were prepared using the FIB from the areas of interest. Only three lamellas survived the final thinning are available for TEM analysis with one (grid 1A) from the center region and two (grid 2A and grid 2B) from the Zr/U-Mo interface region. Detailed microstructural characterization was performed using a 200 kV JEOL-2010 TEM/STEM system equipped with a LaB_6 filament, a Gatan UltraSacn-1000 digital camera for imaging and a Bruker Si drift detector for composition analysis with Energy Dispersive Spectroscopy (EDS). The TEM selected area diffraction (SAD) patterns from the major zones were used for structure analysis. The Java-version Electron Microscopy Simulation (JEMS) software developed by Stadelmann was used to assist in identifying the phases and indexing the diffraction patterns [12].

3. Results and discussion

A comparison of SEM images between the fresh and the irradiated fuel foil is shown in Fig. 2. The fresh U-10Mo fuel foil with Zr barrier layers on the left was used to fabricate the monolithic fuel plate that went through the irradiation in ATR. The irregular interface between U-Mo foil and Zr barrier layer is resulted from the hot rolling of the relative soft Zr against the U-Mo foil. The fuel foil thickness increases from ~250 μm of the fresh condition to ~440 μm of the irradiated condition, corresponding to a fuel swelling of approximately 76%. Since the polishing of this irradiated fuel sample was done manually in a glovebox, surface smearing effect on the highly radioactive fuel with high porosity microstructure can be severe that makes it extremely challenging to obtain pristine microstructural and microchemistry information using a standalone SEM system. However, a FIB-SEM dual-beam system can provide much better images of the freshly sectioned surface for the high porosity microstructure for SEM analysis as shown in Fig. 3. The image on the left shows the U-10Mo/Zr/Al 6061 interface region for SEM analysis and the image on the right reveals the microstructure in the U-10Mo that is selected for TEM lamella preparation for further analysis. Note the magnification for the image on the right is double of that of the left image and it shows the general microstructure consists of a high concentration of large bubbles (>1 μm) and solid fission product precipitates (SFPP) inside these bubbles. Interlinking of the large bubbles is evident. There is still significant fraction of the volume consisting of relatively small bubbles (<200 nm).

Even using a FIB, the TEM sample preparation of the high burn-up fuel can still be extremely challenging because these samples with ~76% swelling tend to break apart before finishing the final thinning to be transparent to 200 kV electron beam for analysis. The internal stress in the sample could also cause sample local bending and buckling when the TEM lamella thickness is significantly reduced. As a result of these challenges, the TEM lamella sample often ends up with missing piece and only very limited area

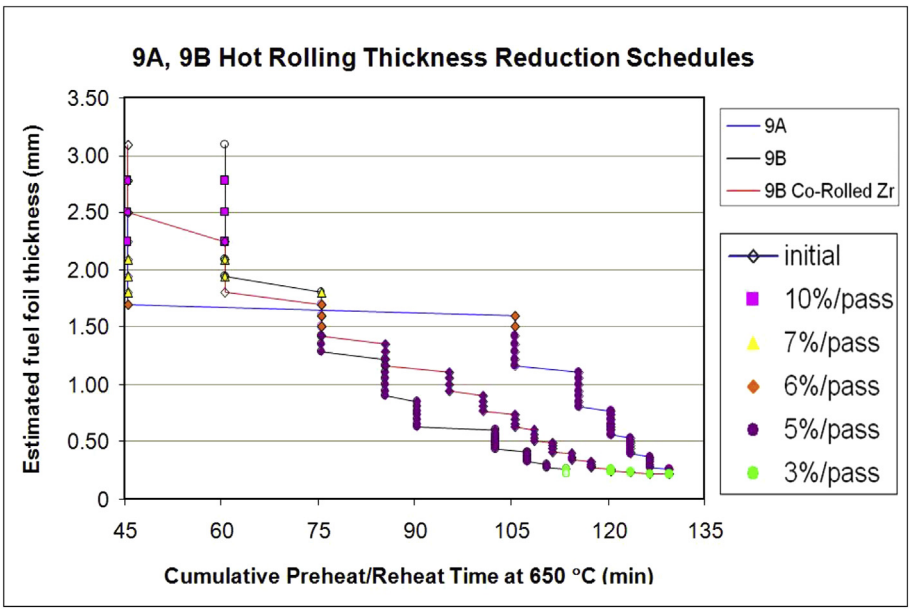

Fig. 1. Rolling schedules used to fabricate foils for irradiation in the RERTR-9A and RERTR-9B experiments. The U-10Mo foil in L1P09T was exposed to the scheduled labeled "9B Co-Rolled Zr".

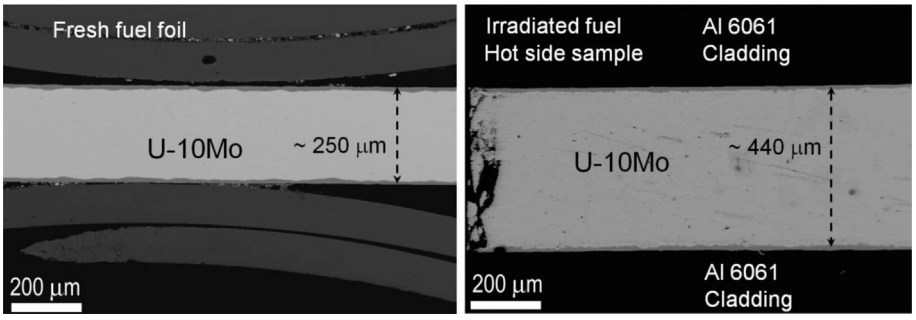

Fig. 2. SEM images comparing the fuel foil thickness of the fresh fuel (left) and the irradiated fuel (right) at a fission density of 9.8×10^{21} fission/cm^3 with a fuel swelling of 76%.

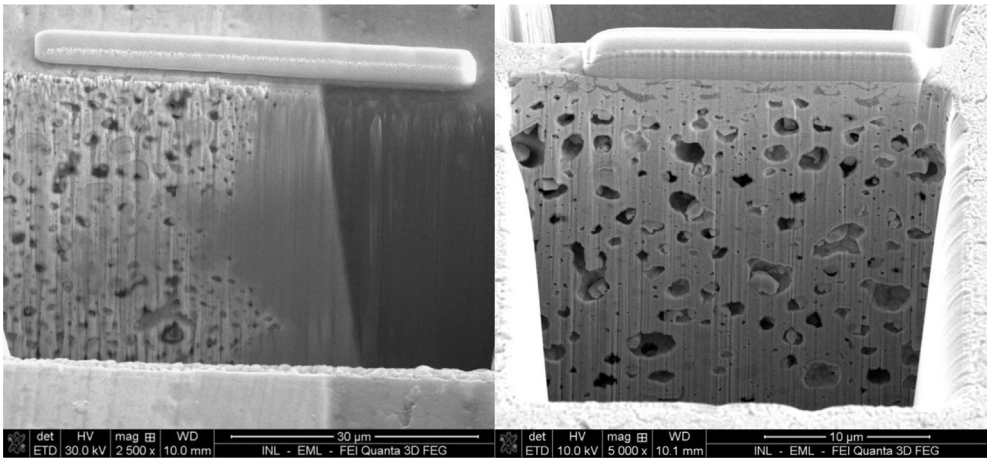

Fig. 3. FIB-SEM images of irradiated U-10Mo fuel microstructure revealing the interface region of U-10Mo/Zr/Al-6061 (left, × 2500) and the U-10Mo fuel interior (right, × 5000).

of the remaining part is thin enough for TEM characterization. TEM low magnification images of the whole lamella view of the three samples characterized in this work are shown in Fig. 4. The sample on the left is from the centerline of the U-Mo fuel foil and the samples in the middle and right are from the U-Mo and Zr barrier interface region.

For sample Grid 1A from the centerline region of the U-Mo fuel, the high magnification TEM image reveals the subdivided grains

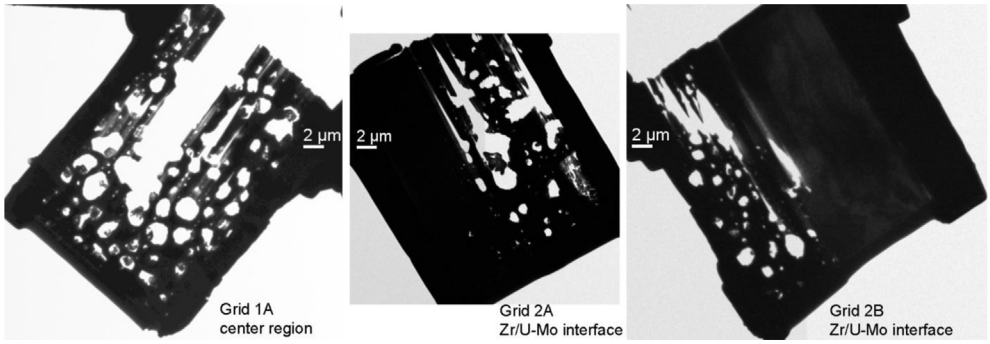

Fig. 4. TEM low magnification images of the whole lamella view for the samples used for microstructural characterization with the left from fuel center region and the middle and the right from Zr/U-Mo interface region.

along with the images of selected area diffraction (SAD) showing bcc zone patterns for U-Mo as shown in Fig. 5. The original large grains (typically ~ 5 μm) subdivided into smaller grains (100–300 nm). The size and morphology of these subdivided grains at 9.8 × 10^{21} fission/cm^3 are similar to that at fission density of 6.3 × 10^{21} fissions/cm^3 [8]. It appears that for the subdivided small grains no further grain subdivision occurs at fission density greater than ~6.3 × 10^{21} fissions/cm^3. The SAD patterns from zone [102] and [112] confirm the bcc crystalline structure of U-Mo with lattice constant estimated from SAD to be 0.349 nm, in general agreement with 0.3413 nm for the unirradiated U-10Mo within the measurement uncertainty. The ring pattern in SAD is attributed to surface oxidation of U-Mo. The estimated lattice constant from the oxide ring is 0.549 nm, in good agreement with the literature data of 0.5470 nm for UO_2 [13]. Most part of the boundaries of the subdivided grains is quite clean without bubbles. Some of the large bubbles seem to be located at triple junction which could be the region of high stress concentration.

The high magnification TEM images of Grid 1A from the area without large bubbles reveal a high concentration of small bubbles in random arrangement as shown in Fig. 6 where these small bubbles are confirmed as white dots and black dots in the imaging condition of under-focus (left) and over-focus (right), respectively. The estimated bubbles size is ~2 nm, smaller than the average size of the GBS bubbles (~3.5 nm) typically observed at lower fission densities [7,8]. This observation is quite a surprise. From the previous investigations it was speculated that, at very high fission densities (>7 × 10^{21} fissions/cm^3) where the microstructure is dominated with large bubbles, small bubbles will be wiped out and all the additional fission gas atoms produced in the fuel will feed to the large bubbles and consequently result in more aggressive fuel swelling. A high concentration of small bubbles found at very high fission density in this work indicates that a high burn-up U-Mo fuel grain is still capable of maintaining high gas inventory with these highly pressurized fine bubbles. This observation questions the mechanism for aggressive swelling with large bubbles at the high fission densities, whether it is driven by fission gas or by a combination of vacancy partitioning and fission gas. It is possible that, while fission gas may continue playing a critical role in bubble nucleation, the aggressive growth of large bubbles may be driven mainly by vacancy partitioning. Although the nominal irradiation temperature based on estimation from the calculation is relatively low, the development of large bubbles (>1 μm) filled with Xe gas in fuel region could significantly degrade thermal conductivity of the fuel, raise local temperature and increase vacancy mobility. The point defect concentration and flux in U-Mo fuel from fission fragment bombardment can be significantly higher than that typically seen in metallic structural materials from fast neutron

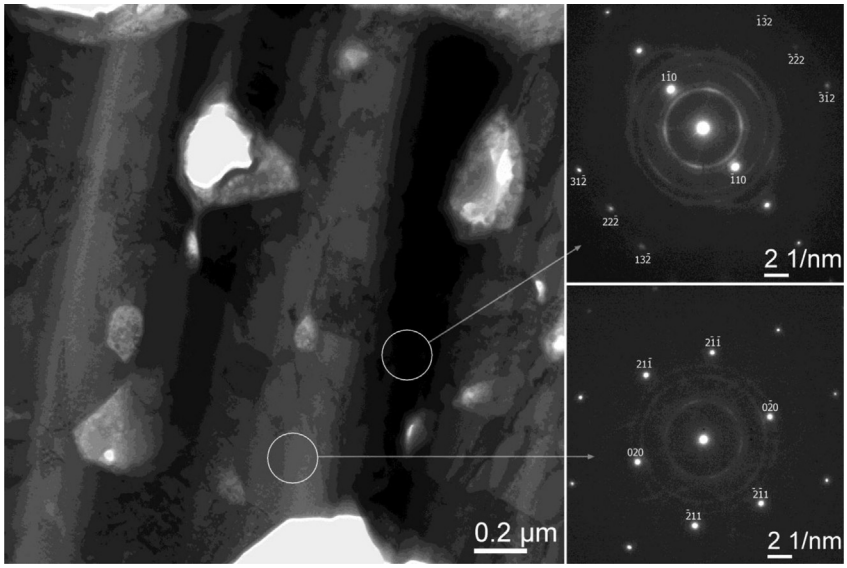

Fig. 5. TEM image of irradiated U-Mo fuel from the center region revealing subdivided grains (left) and the SAD zone patterns of bcc U-Mo (right) at zone [112] (top) and [102] (bottom). Note there is no evidence of preferential bubble accumulation at subdivided grain boundaries. The ring patterns are from the surface oxide of UO_2.

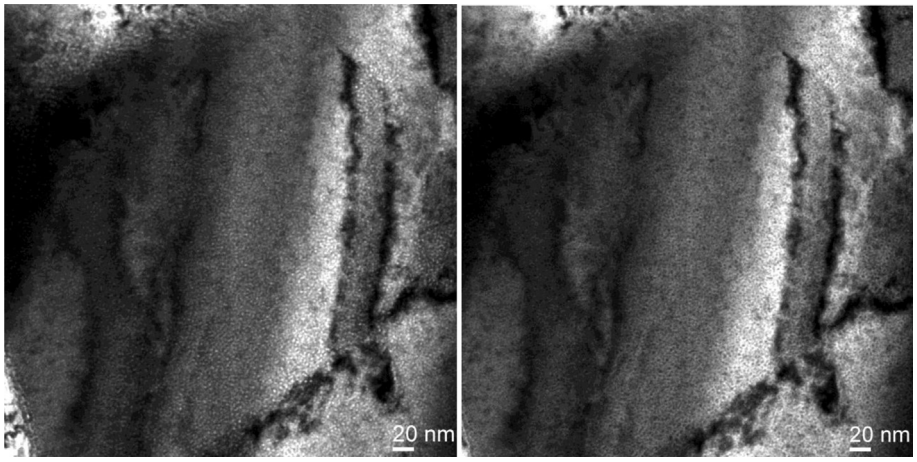

Fig. 6. High magnification TEM image of small bubbles from sample Grid 1A of fuel center region under the imaging condition of under-focus (left) and over-focus (right). The estimated bubble size is ~2 nm.

irradiation, therefore the role of vacancies in U-Mo fuel swelling at high fission density is speculated to be significant and possibly the main driving mechanism.

Fig. 7 shows a small pocket of GBS bubbles oriented at zone [011] in the upper left corner with average bubble size and fcc superlattice constant of ~3 nm and ~11 nm, respectively, consistent with the measurement at lower fission density of ~3×10^{21} fissions/cm^3. It is not clear whether these are residual GBS or newly developed GBS. This finding is also unexpected since only few scattered pockets of residual GBS are found at 6.3×10^{21} fissions/cm^3 and it is hard to believe that these pockets of residual GBS could survive at 9.8×10^{21} fissions/cm^3. If the observed pocket of GBS is newly developed at very high fission densities, it may be possible that only those regions with relatively low stress concentration capable to develop GBS. At very high fission densities, the low stress concentration regions are significantly reduced and rarely exist, therefore only few scattered pockets of GBS can be found although high concentration small bubbles distributed randomly seem to be quite stable under the given condition.

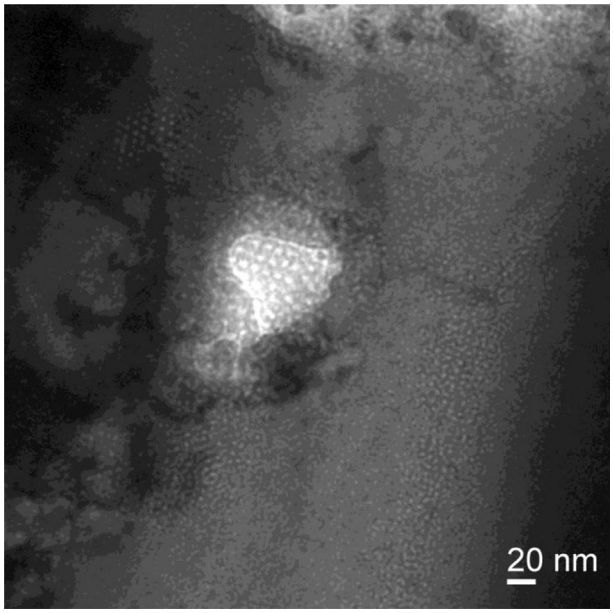

Fig. 7. TEM image of sample Grid 1A at high magnification showing small pocket of superlattice bubbles in the upper left corner.

Fig. 8 shows the STEM image from sample Grid 1A with areas marked for EDS composition analysis. The results from the measurement are listed in Table 1. Fuel matrix composition from fuel centerline region of the irradiated U-Mo fuel (spot 1–6) mainly consists of U (~60 at.%), Mo (~28 at.%) and Zr (~6.1 at.%). The nominal atomic concentration of Mo for U-10Mo in the unirradiated condition is estimated to be 21.7 at%. The significant increase in Mo content by ~6 at.%, comparable to ~6 at.% of Zr, is believed to be from the high fission yield that is similar for Mo (0.234 at./fission) and Zr (0.267 at./fission) for ^{235}U fission under light water reactor neutron spectrum [14]. It appears that both Mo and Zr produced from fissions are mostly kept in solution in U-Mo fuel since both are not detected in the SFP inclusions inside the large bubbles. High Xe content (>4 at.%) is detected in many SFP inclusions inside the large bubbles. It was noticed that, when converging the electron beam on some SFP inclusions during TEM analysis, the embedded small gas bubbles expand and burst rather quickly. How the Xe gas gets trapped in the SFP inclusion inside the large bubble is not fully understood. Large amount of Sr (>20 at.%) and Ba (>9 at.%) are also detected in the SFP inclusions inside the large bubbles along with small amount of Nd (>1 at.%). Note that EDS measurement generally only provides qualitative composition estimate for relative comparison. The associated relatively uncertainty could be up to 10%. Caution has to be taken when using the EDS data to draw definitive conclusion about absolute composition.

Fig. 9 shows the STEM image of irradiated fuel matrix where the green line marks the EDS elemental line scan for uranium, molybdenum and zirconium. One hundred data points were collected in 10 min and analyzed to generate this composition profile over a distance of 6.5 μm with a probe size of 25 nm. The resultant plot in at.% is shown on the right where Zr (~7 at.%) is in agreement with the estimated Zr production of approximately ~ 6 at.% at this fission density. The consistent Zr profile indicates fission is relatively uniform while the gradually change of Mo profile may be related to Mo variation typically found in the fresh fuel. Since the STEM probe size in this work is 25 nm, approximately 40 times smaller than a typical ~1 μm probe size in EDS/WDS in a SEM or EPMA system, the fluctuation of the composition profile shown in the plot is considered to be real as a result of high spatial resolution EDS analysis in TEM. The elemental mapping of the area at the arrow of the green line is shown in Fig. 10. The mapping takes 1 h to finish and it clearly shows that the SFP precipitates in the large bubbles are dominated by Sr. It is interesting to see that the highest Nd concentration is at

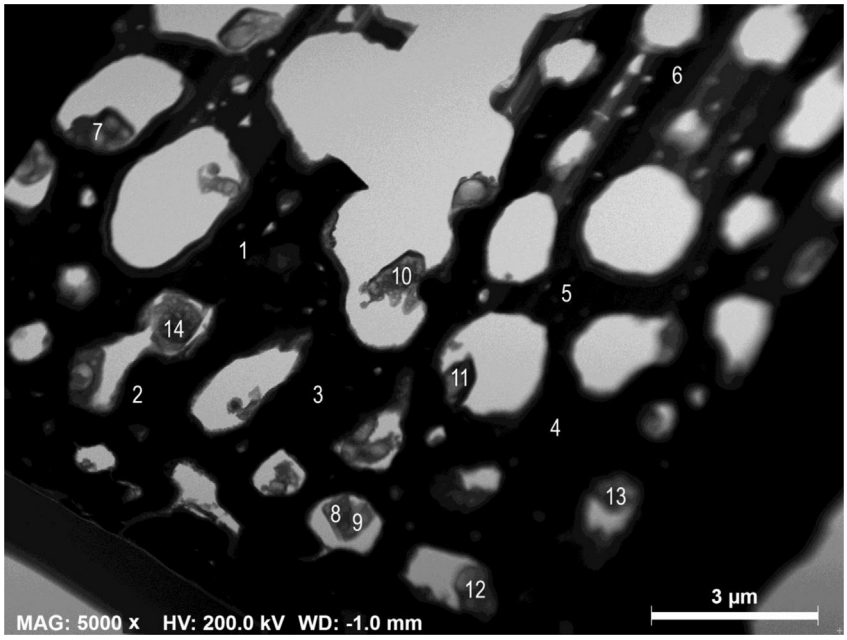

Fig. 8. STEM low magnification image of sample Grid 1A from fuel center region with areas marked for composition analysis in EDS spot mode.

Table 1
EDS measurement (at.%) of irradiated U-Mo fuel (Grid 1A) at locations shown in Fig. 8.

Location	Zr	Mo	U	Other element in at%
1	7.9	29.5	54.9	Ce_6.9, Y_0.8
2	5.9	26.9	58.6	Ce_7.8, Y_0.8
3	5.8	27.6	61.3	Ce_5.4
4	5.8	29.5	59.2	Ce_5.1
5	6.7	29.2	60.3	Ce_3.8
6	4.2	25.7	65.2	Ce_4.9
7	9.0	10.9	21.6	Ba_23.7, Sr_20.8, Ce_5.7, Y_3.4, Nd_2.4, Te_2.7
8	11.5	0	0.9	Sr_58.0, Ba_22.3, Xe_5.7, Nd_1.2
9	18.8	0	1.2	Sr_43.9, Ba_29.9, Xe_4.3, Nd_2.0
10	38.4	0	0.6	Sr_37.8, Ba_13.7, Xe_8.4, Nd_1.1
11	21.6	0	1.8	Sr_47.1, Ba_20.2, Xe_6.4, Nd_2.9
12	10.9	0	2.4	Sr_56.4, Ba_23.9, Xe_5.2, Nd_1.2
13	10.0	0	8.8	Sr_53.6, Ba_23.8, Nd_3.9
14	46.9	0.5	0.9	Sr_31.2, Ba_9.3, Xe_8.9, Nd_2.4

the surface region of large bubbles. Nd distribution in oxide fuel can be used as a marker for fission density distribution since it ties to oxygen to form immobile Nd-O compound. Care has to be taken when using Nd to evaluate the fission density uniformity in metal fuel since it can diffuse towards large bubbles likely due to the temperature gradient. Mo and Zr appear remained in the fuel matrix and are barely detectable in the SFP precipitates inside the large bubbles. It suggests that Zr may be used as a marker for evaluation of fission density uniformity in metal fuels not containing Zr as a fuel alloy element or transmutation product. Ba distribution appears relatively uniform in both fuel matrix and SFP inclusions. It seems fuel matrix still retains significant amount of Xe, in agreement with the observed high concentration of fine bubbles shown in Fig. 6.

In addition to the irradiated microstructure in the U-Mo fuel zone, the microstructural development at U-Mo fuel foil and Zr

Table 2
EDS measurement (at.%) of irradiated U-Mo fuel (Grid 1A) at locations shown in Fig. 11.

Location	Zr	Mo	U	Xe	Other element in at%
1	99.5	0.4	0.1	–	A sign – means not detected
2	99.5	0.5	0	–	
3	94.1	2.0	0.8	3.1	
4	98.6	1.3	0.1	–	
5	91.3	2.3	2.2	4.3	
6	95.0	1.6	0.2	1.5	
7	79.0	7.1	11.1	2.9	
8	57.9	20.5	18.8	2.8	
9	15.7	22.3	60.2	1.8	
10	41.9	4.2	12.7	–	Ga_34.6, Al_7.7
11	33.3	1.3	0	24.5	Sr_29.5, Ba_11.4
12	91.9	3.1	1.4	–	Ba_1.9, Nd_1.7
13	71.8	7.3	17.4	–	Sr_0.6, Ba_1.9, Ce_1.1
14	11.9	16.9	71.2	–	
15	8.1	21.4	69.8	0.7	
16	19.8	1.9	20.7	2.0	Sr_20.7, Ba_13.3, Nd_11.8, Ce_8.3, Y_3.6
17	76.9	3.7	3.7	–	Sr_0.7, Ba_8.4, Nd_2.8, Ce_1.6
18	6.9	2.6	3.6	4.1	Sr_7.8, Nd_44.9, Ce_18.1, Te_6.0, Y_4.1, Ba_1.9

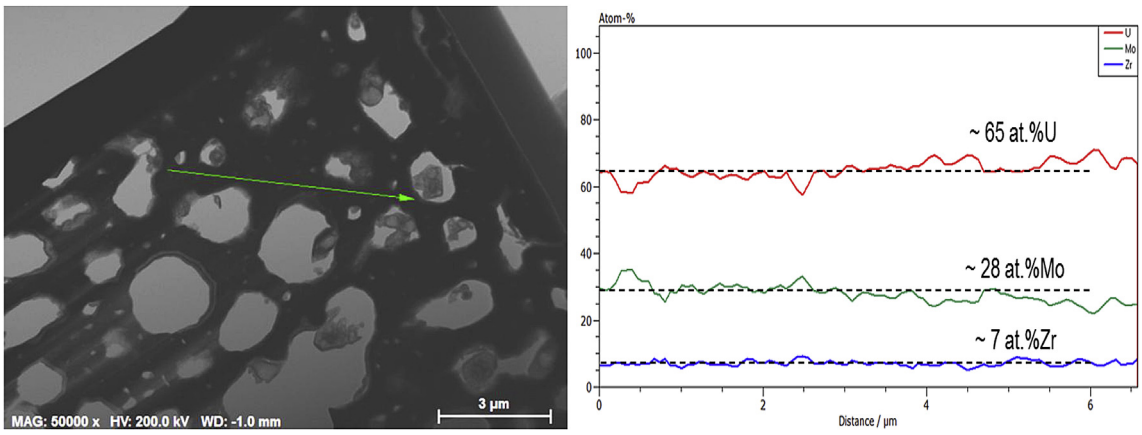

Fig. 9. STEM image of irradiated U-Mo fuel from center region (left) with the green line indicating where EDS line scan was performed. The composition line profiles in at.% are shown in the plot (right) with dashed lines for the estimated mean values. (For interpretation of the references to colour in this figure legend, the reader is referred to the web version of this article.)

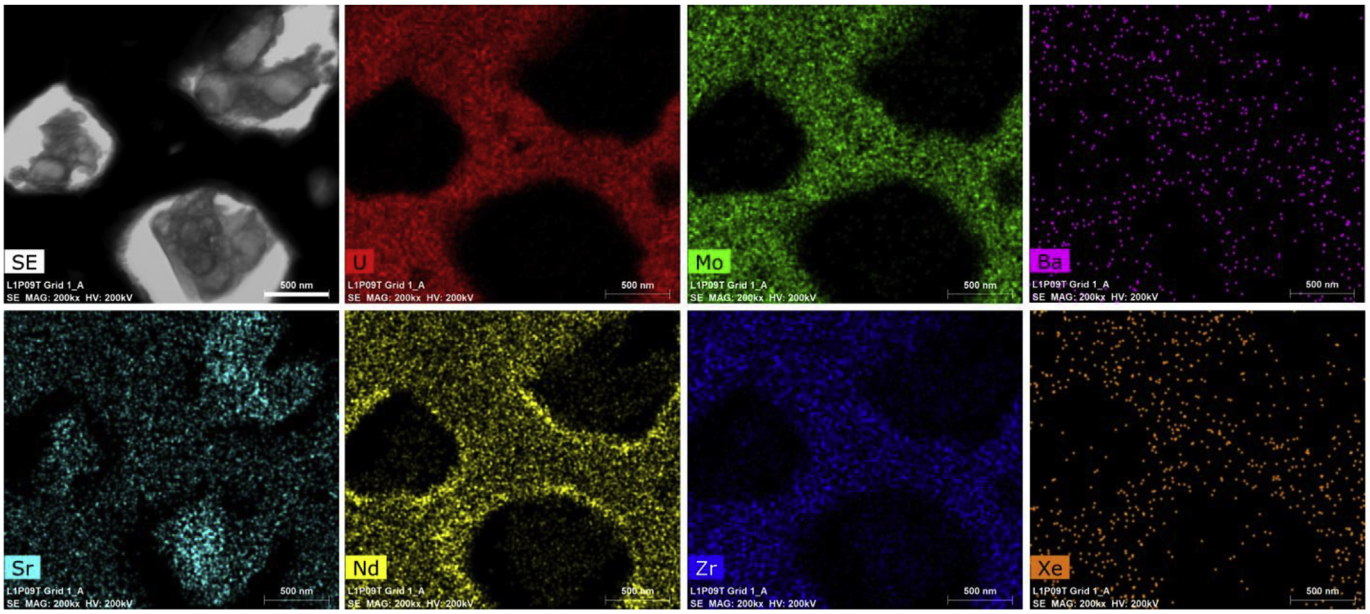

Fig. 10. EDS elemental mapping from the fuel centerline region of the irradiated U-10Mo fuel (Grid1A) at the fission density of 9.8 × 10^{21} fissions/cm^3 reveals fission product distribution in area with large bubbles. The scale bar is 500 nm.

barrier interface region can also strongly impact the performance of a monolithic fuel plate. Fig. 11 shows a low magnification STEM image (left) of the interface region from sample Grid 2A with areas marked for EDS analysis (see Table 2) along with a TEM image (right) showing the details of a SFP inclusion marked as feature C. Points 1–6 and 12 have Zr content greater than 91 at%, representative of a Zr barrier layer. Points 9, 14 and 15 have high U and Mo content, likely on the U-Mo fuel side. Points 3, 5–9 and 15 show detectable amount of Xe in both the Zr barrier and the U-Mo fuel matrix. The SAD diffraction pattern from area A, B and area 1–6 with uniform contrast in Zr barrier layer reveals a ring pattern of nanostructure. The estimated grain size of the nanocrystalline Zr region is in the range of 50–100 nm. The exact cause of forming a nanograin region in the Zr diffusion barrier is not well understood. The magnified view of the SFP inclusion shows a high concentration of trapped Xe gas bubbles. When the electron beam is converged on this SFP inclusion, the trapped gas bubbles coarsen and grow rapidly under the beam heating as shown in Fig. 11 (right) where a large bubble (~90 nm) adjacent to a bubble depleted zone can be seen near the middle-left.

A low magnification STEM image of the interface region from a different FIB sample (Grid 2B) and the results for an EDS line scan of the major elements (U, Mo and Zr) (in at.%) are shown in Fig. 12. The length of the line scan and the collection time is 11.6 µm and 10 min, respectively. Near the end of the line scan path, the local composition for U, Mo and Zr are in general agreement with the averaged values for fuel interior as shown in Fig. 9. Unlike the nanocrystalline Zr in sample Grid 2A shown in Fig. 11, the SAD patterns from Zr in sample Grid 2B clearly reveal spot patterns of crystalline hcp structure. Although the exact cause of the difference in the observed Zr structure near Zr/U-Mo interface is not clear at this point, it has been noticed that nanocrystalline Zr is also identified as a general microstructural feature in other irradiated monolithic fuel plate with a Zr diffusion barrier layer. As shown in the composition line profile in Fig. 12, there is no clear evidence showing the presence of UZr_2 and Mo_2Zr interaction phases at the

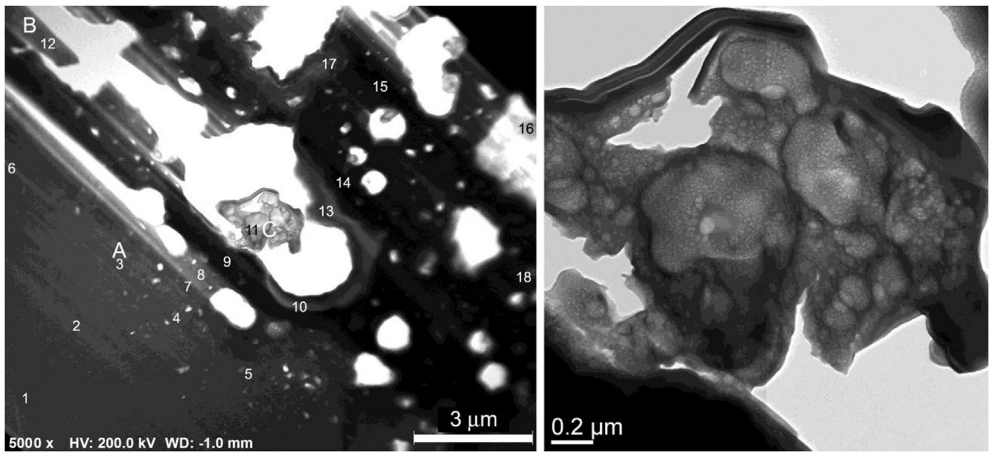

Fig. 11. STEM image of U-Mo and Zr interface region for sample Grid-2A at low magnification (left) and TEM image of detailed microstructure of feature C (right) showing Xe bubbles trapped in the inclusion inside a large bubble.

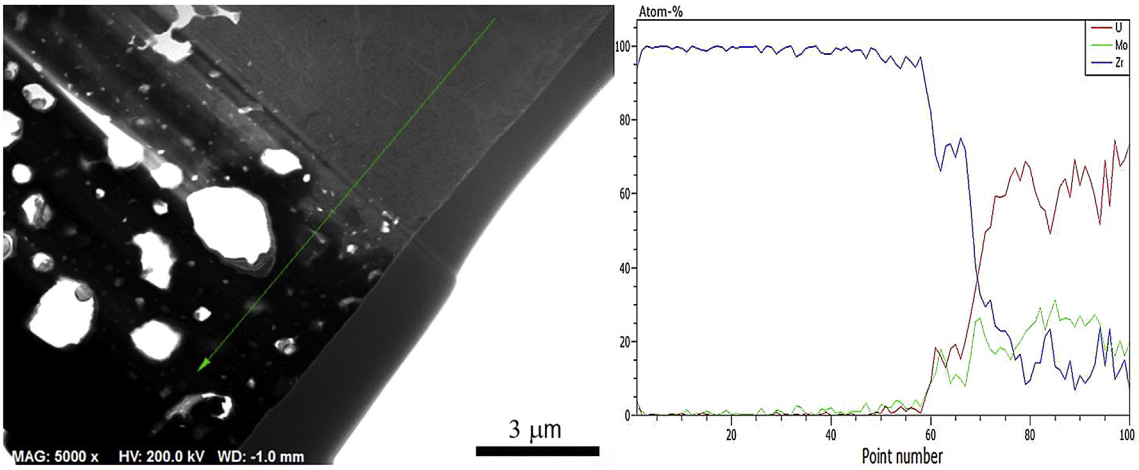

Fig. 12. STEM image of U-Mo and Zr interface region for sample Grid-2B at low magnification (left) and the EDS line scan showing composition profile for Zr, U and Mo across the interface (right).

Zr/U-Mo interface region at the specified high fission density, although both are found in the fresh fuel from the work by Perez [15].

The measured high swelling of ~76% in U-Mo fuel is anticipated at this very high fission density of 9.8×10^{21} fissions/cm^3 knowing that the atomic concentration of U-10Mo fresh fuel is 5.03×10^{22} atoms/cm^3 and about 25% uranium atoms are consumed by fissions. The EDS measurement for Mo and Zr are in general agreement with the estimated fission yield for the given fission density. However, some microstructural features are not expected to be present at this very high fission density based on the previous TEM works of the irradiated U-7Mo fuels at fission densities up to ~6.3×10^{21} fissions/cm^3.[reference] These findings include: (1) a high concentration of fine bubbles (~2 nm) in the fuel matrix; (2) no additional changes in the U-Mo subdivided grains over what has been observed for fuels irradiated to ~ 6×10^{21} fissions/cm^3; (3) the observation of small pockets of GBS bubbles in the U-Mo fuel, and (4) a different structure for the Zr diffusion barrier layer (nanocrystalline vs. crystalline) compared to actual Zr/U-Mo interface region, as revealed by SAD patterns (ring vs. spot pattern). The first finding may be the most significant since it indicates that a different mechanism for swelling behavior under very high fission density may need to be considered where the contribution from vacancies could be dominant. More extensive TEM and SEM investigation are required to have a comprehensive understanding of the mechanisms governing the microstructural development of irradiated monolithic fuel at very high fission densities.

4. Summary

TEM characterization of a monolithic U-10Mo/Zr/Al6061 fuel plate (L1P09T) irradiated to 9.8×10^{21} fissions/cm^3 at the estimated fuel centerline temperature of 141 °C (BOL) and 194 °C (EOL) with a fuel swelling of ~76% is carried out. The region at the fuel centerline revealed irradiated microstructure dominated with large bubbles up to ~3 μm. The interlinking of bubbles is evident. The feature of grain subdivision looks similar to that at ~6×10^{11} fissions/cm^3, and no further subdivision for the subdivided grains at higher fission densities is observed. A high concentration of randomly distributed small bubbles (~2 nm) are found in the U-Mo fuel matrix at very high fission density, contrary to the previous speculation that the small bubbles will disppear, and newly-produced fission gas atoms will feed the large bubbles at very high fission densities (>7×10^{11} fissions/cm^3). Scattered small pockets of GBS fine bubbles are still present in the U-Mo fuel at very high fission density.

Acknowledgments

Acknowledgment is given to the INL Hot Fuel Examination Facility staff for producing the small sample from precision cutting of the irradiated fuel plate L1P09T. This work was supported by the U.S. Department of Energy, Office of Material Management and Minimization, National Nuclear Security Administration, under DOE-NE Idaho Operations Office Contract DE-AC07-05ID14517. This manuscript was authored by a contractor for the U.S. Government. The publisher, by accepting the article for publication, acknowledges that the U.S. Government retains a nonexclusive, paid-up, irrevocable, worldwide license to publish or reproduce the published form of this manuscript, or allow others to do so, for U.S. Government purposes.

References

[1] C.A.W. Peterson, W.J. Steele, S.L. DiGiallonardo, Isothermal Transformation Study of Some Uranium-base Alloys, Report: UCRL-7824, Metals, Ceramics, and Materials, UC-25, TID-4500, 34th Ed., Lawrence Radiation Laboratory, Livermore, California, August, 1964.
[2] P.E. Repas, R.H. Goodenow, R.F. Hehemann, Trans. ASM 57 (1964) 150–163.
[3] A. Leenaers, S. Van den Berghe, E. Koonen, C. Jarousse, F. Huet, M. Trotabas, M. Boyard, S. Guillot, L. Sannen, M. Verwerft, J. Nucl. Mater 335 (2004) 39–47.
[4] D.D. Keiser Jr., J.F. Jue, C.R. Clark, U-Mo Foil/Cladding Interactions in Friction Stir Welded Monolithic RERTR Fuel Plates, in: Proceedings of the 26th International Meeting on Reduced Enrichment for Research and Test Reactors (RERTR), Cape Town, South Africa, October 29–November 2, 2006.
[5] H.J. Ryu, Y.S. Kim, G.L. Hofman, D.D. Keiser Jr., Characterization of the Interaction Products in U-Mo/Al Dispersion Fuel from In-Pile ad Out-of-Pile Tests, in: Proceedings of the 26th International Meeting on Reduced Enrichment for Research and Test Reactors (RERTR), Cape Town, South Africa, October 29–November 2, 2006.
[6] S. Van den Berghe, W. Van Renterghem, A. Leenaers, J. Nucl. Mat. 375 (2008) 340–346.
[7] J. Gan, D.D. Keiser Jr., D.M. Wachs, A.B. Robinson, B.D. Miller, T.R. Allen, J. Nucl. Mat. 396 (2010) 234–239.
[8] J. Gan, D.D. Keiser Jr., B.D. Miller, A.B. Robinson, J.F. Jue, P. Medeved, D.M. Wachs, J. Nucl. Mat. 424 (2012) 43–50.
[9] J. Gan, B.D. Miller, D.D. Keiser Jr., A.B. Robinson, J.W. Madden, P.G. Medvedev, D.M. Wachs, Microstructural characterization of irradiated U-7Mo/Al-5Si dispersion fuel to high fission density, J. Nucl. Mat. 454 (2014) 434–445.
[10] D.M. Perez, M.A. Lillo, G.S. Chang, G.A. Roth, N.E. Woolstenhulme, D.M. Wachs, RERTR-9 Irradiation Summary Report, Idaho National Laboratory Report INL/EXT-10-18421, May 2011.
[11] Hakan Ozaltun, Pavel Medvedev, Effects of the foil flateness on the stress-strain characteristics of U-10Mo alloy based monolithic mini-plates, in: Proceeding of ASME 2014 International Mechanical Engineering Congress and Exposition, 6B, Energy, Novermber 14–20, 2014.
[12] P. Stadelmann, http://cimewww.epfl.ch/people/stadelmann/jemsWebSite/jems.html.
[13] P. Goel, N. Choudhury, S.L. Chaplot, J. Nucl. Mat. 377 (2008) 438–443.
[14] Henri Bailly, Denise Menessier, Claude Prunier, The Nuclear Fuel of Pressurized Water Reactors and Fast Reactors design and Behavior, Lavoisier Publishing, 1999.
[15] E. Perez, B. Yao, D.D. Keiser, Y.H. Sohn, J. Nucl. Mat. 402 (2010) 8–14.